Journal of Lasers in Medical Sciences

J Lasers Med Sci. 2025;16:e65

Original Article

http://journals.sbmu.ac.ir/jlms

doi 10.34172/jlms.2025.65

Experimental Investigation of the Effects of Photobiomodulation Therapy on the Viability, Migration, and Gene Expression of Human Gingival Fibroblasts

Jaber Zafari[1], Danial Khayatan[2,3], Leila Mohaghegh Shalmani[1], Hossein Vazini[4], Fatemeh Javani Jouni[5*]

[1]Department of Pharmacology and Toxicology, TeMS.C., Islamic Azad University, Tehran, Iran
[2]Laser Application in Medical Sciences Research Center, Shahid Beheshti University of Medical Sciences, Tehran, Iran
[3]GI Pharmacology Interest Group (GPIG), Universal Scientific Education and Research Network (USERN), Tehran, Iran
[4]Department of Nursing, Ha.C., Islamic Azad University, Hamedan, Iran
[5]Department of Biochemistry and Biophysics, TeMS.C., Islamic Azad University, Tehran, Iran

***Correspondence to**
Fatemeh Javani Jouni,
Email: Javani@iau.ac.ir

Received: July 19, 2025
Accepted: September 30, 2025
ePublished: December 9, 2025

Abstract

Introduction: The wound healing process is a complex cascade of events crucial for tissue repair, involving cellular and molecular mechanisms. Disruptions can lead to chronic wounds. Photobiomodulation therapy (PBMT) utilizing red and near-infrared light has emerged as a promising modality. This study aimed to evaluate the effects of PBMT with 650 and 810 nm lasers, alone and in combination, on human gingival fibroblasts (HGFs), focusing on cell viability, migration, cytokine production, and expression of genes (TNF-α, IL-6, IFN-γ, VEGF, Fibronectin, Collagen I, MMP1, and MMP8).

Methods: Human gingival fibroblasts were irradiated with 650 and/or 810 nm lasers at varying doses. MTT assay, scratch assay, cytokine profiling (IL-6, IFN-γ, TNF-α), and real-time PCR were performed.

Results: PBMT significantly enhanced cell viability and migration, with combined 650 and 810 nm showing the most pronounced effects. Cytokine profiling and gene expression revealed wavelength-specific responses: upregulation of VEGF, Fibronectin, and Collagen I, and differential modulation of IL-6, TNF-α, IFN-γ, MMP1, and MMP8.

Conclusion: PBMT exerts wavelength-dependent effects on fibroblast activity, with synergistic benefits observed under combined irradiation. These findings highlight PBMT's potential for wound healing and regenerative medicine.

Keywords: Wound healing; Photobiomodulation therapy (PBMT); Human gingival fibroblast.

Introduction

Wound healing is a multifaceted process that unfolds in distinct stages, including hemostasis, inflammation, tissue proliferation, and remodeling. These phases encompass a series of intricate events, including clot formation, cellular migration, chemotaxis, phagocytosis, angiogenesis, and collagen deposition, leading to granulation tissue formation.[1] However, disruptions in this highly orchestrated process can result in chronic wounds, which are prevalent among individuals with vascular diseases or diabetes, presenting substantial challenges for healthcare systems worldwide. Despite significant advancements in wound care, the treatment of non-healing wounds continues to pose a significant challenge, necessitating further exploration and innovative therapeutic approaches. In the realm of wound healing, red light and NIR (Near Infrared) light, typically emitted by low-power lasers or LEDs within the 600 to 900 nanometer range, have emerged as promising modalities with beneficial effects on cellular and tissue injury models.[2] Studies have demonstrated that such light radiation can enhance mitochondrial metabolism, stimulate wound healing, and promote angiogenesis across various tissues, including skin, bone, nerves, and skeletal muscles. By activating cellular signaling pathways, red light and NIR light augment immediate adenosine triphosphate (ATP) production and bolster DNA and RNA activity, thereby exerting favorable effects on cellular function and tissue repair. A growing body of research on low-power lasers has underscored their potential in facilitating tissue repair and regeneration, offering promising avenues for therapeutic intervention in wound healing processes.[3,4] Recent investigations have pinpointed specific wavelengths within the 600 to 900 nanometer range, such

Please cite this article as follows: Zafari J, Khayatan D, Mohaghegh Shalmani L, Vazini H, Javani Jouni F. Experimental investigation of the effects of photobiomodulation therapy on the viability, migration, and gene expression of human gingival fibroblasts. *J Lasers Med Sci.* 2025;16:e65. doi:10.34172/jlms.2025.65.

as 750-770, 660-690, 610-625, and 815-860 nanometers, as exhibiting optimal therapeutic effects. NIR-LED devices have garnered attention as viable therapeutic tools for a variety of soft tissue injuries, including wounds caused by infection, reduced blood flow, and low oxygen levels, in both human and animal models. The way it works is through the increased activity of cytochrome C oxidase and ATP production, as evidenced in primary cultures of visual cortex neurons treated with inhibitors like tetrodotoxin, potassium cyanide (KCN), or sodium azide (NaN3). Additionally, recent studies have highlighted the efficacy of a 670-nanometer LED light source in tissue repair and in mitigating certain types of damage, such as the toxic effects of methanol on the retina.[5-7] Against this backdrop, the current research aimed to address the knowledge gap by evaluating the wound-healing effects of photobiomodulation therapy (PBMT) on human gingival fibroblasts (HGF).[8] Through meticulous experimentation employing the MTT method ((3-(4,5-dimethylthiazol-2-yl)-2,5-diphenyltetrazolium bromide)) and a scratching technique, this investigation aimed to elucidate the potential therapeutic effects of photobiomodulation exposure at 650 and 810 nanometers across various durations and intensities.[9] By conducting these experiments under controlled laboratory conditions, this research aimed to uncover detailed insights into the mechanisms by which photobiomodulation influences wound healing in human gingival fibroblasts. Furthermore, by clarifying the clinical implications of these findings, particularly in the context of oral health and dental procedures, this study intended to support the advancement of enhanced therapeutic approaches for wound healing and regenerative medicine. The present study specifically investigated cytokines (IL-6, TNF-α, IFN-γ) and genes related to extracellular matrix remodeling and angiogenesis (Collagen I, Fibronectin, VEGF, MMP1, and MMP8) in HGF cells. The objective was to elucidate how PBMT at 650 nm and 810 nm, alone and in combination, influences these targets and contributes to wound healing.

Methods and Materials

Cell Culture

Human gingival fibroblasts (HGF), obtained from the Pasteur Institute of Iran, were cultured in Dulbecco's Modified Eagle Medium (DMEM) supplemented (Sigma-Aldrich, St Louis, MO, USA) with 10% fetal bovine serum (FBS) in sterile flasks. The cells were maintained in a humidified incubator at 37°C with 5% CO2 and subcultured every 2-3 days upon reaching 70-80% confluency.

Laser Treatment

This study utilized two distinct lasers: the 650 nm diode Laser (P1 Dental Laser, Pioon, China) and the 810 nm Elexxion nanolaser (Germany) (Table 1).

Table 1. Technical specifications of different lasers

Name of laser company	Ploon	Elexxion nano
Wavelength	650	808 ± 10
Power output (mW)	200 ± 20	200 and 900
Energy Density *(J/cm²)	4 and 8	4, 5.4, 8 and 8.1
Time (s)	20, 40	20, 6, 40 and 9
Spot Size (cm²)	1	1
Operation	Continuous	Pulse (16 µs / CW) **

*Energy density was calculated as (Power × Time) / Area
** The Elexxion nanolaser was used in pulsed (16 µs) and continuous-wave (CW) modes as indicated.

Experimental Groups

- Control Group: Cells were maintained in the incubator without exposure to laser treatment for 24 hours.
- Laser (650 nm) Groups: Two groups received energies of 4 or 8 J/cm² and were cultured for 24 hours post-treatment.
- Laser (810 nm) Groups: Four groups received energies of 4, 5. 4, 8 or 8.1 J/cm² and were cultured for 24 hours post-treatment.
- Laser (650 + 810 nm) Groups: Simultaneously, cells were exposed to both wavelengths and divided into two groups. These groups received energies of 6.6 or 8 J/cm² and were cultured for 24 hours post-treatment.

The groups were designed to evaluate dose-response effects at clinically relevant ranges and to compare single with combined wavelength treatment (Table 2).

MTT Assay for Viability

The evaluation of cell viability is fundamental in elucidating the effects of red laser light on human gingival fibroblasts (HGF). To achieve this, we employed the MTT (3-(4,5-dimethylthiazol-2-yl)-2,5-diphenyltetrazolium bromide) assay, leveraging its capability to measure mitochondrial dehydrogenase activity, a marker of viable cells.[10] Upon completion of the laser treatment regimen outlined in Section 2.2, the cultured HGF cells were subjected to the MTT assay to evaluate their viability. Briefly, the cells were seeded into 96-well plates at a predetermined density and allowed to adhere overnight. Following adherence, the cells were exposed to the various laser treatments specified in Section 2.3. Subsequent to the exposure period, the culture medium was aspirated, and MTT solution was added to each well.[11] The plates were then incubated under standard conditions to allow viable cells to metabolize MTT into formazan crystals. After the specified incubation period, typically 3-4 hours, the formazan crystals were solubilized using an appropriate solvent, such as dimethyl sulfoxide (DMSO), to yield a colored solution. The absorbance of the resulting solution, which correlates directly with the number of metabolically

Table 2. Experimental groups in this study

Group name	Time (s)		Power (W)		Intensity (J/cm²)
	650 nm	810 nm	650 nm	810 nm	
Control	-	-	-	-	-
Laser (650 nm)	20	-	0.2	-	4.0
	40	-	0.2	-	8.0
Laser (810 nm)	-	6	-	0.9	5.4
	-	9	-	0.9	8.1
	-	20	-	0.2	4.0
	-	40	-	0.2	8.0
Laser (650+810 nm)	20	20	0.2	0.2	8.0
	6	6	0.2	0.9	6.6

* Spot size was 1 cm² for both devices; energy density was calculated as (Power×Time) / Area

active cells, was measured spectrophotometrically at a wavelength range of 500-600 nm by a microplate reader.[12]

Cell Migration Analysis

Scratch assays are being performed on 48-well plates with 20,000 HGF cells seeded per well to assess their migratory behavior following exposure to red laser light. The procedure involves inducing scratches across the center of each well using a sterile pipette tip, ensuring uniform width and length. Time-lapse imaging commences immediately after scratch induction, capturing images at regular intervals using a phase-contrast microscope equipped with a digital camera.[13] Plates are housed in a live-cell imaging system within a standard cell culture incubator to maintain physiological conditions throughout the imaging process. Subsequent image analysis utilizing software such as NIH ImageJ enables the quantification of scratch closure rates by measuring scratch width at multiple points along its length.[14]

Cytokine Profiling

Cytokine levels, including Interferon-gamma (IFN-γ), Interleukin-6 (IL-6), and Tumor Necrosis Factor-alpha, were explored using the commercial kits from Karmania Pars Gene Company, Kerman, Iran, and based on the manufacturer's guidelines. Briefly, 50 µL of cell supernatant and 50 µL of standards were added to the ELISA plate and incubated for 60 minutes. Then the plates were washed with the washing buffer, and the detection antibody and HRP-AVIDIN were added. After incubation for 60 minutes, the plates were washed. Then the substrate was added. After 15 minutes, the reaction was stopped by the stopping solution, and the optical density (OD) was detected using an ELISA reader (Dana Tashkhis, Tehran, Iran) at 450 nm.

Gene expression analysis

Using real-time PCR, the fold changes in mRNA expression levels of genes, including Tumor Necrosis Factor-alpha (TNF-α), Interleukin-6 (IL-6), Interferon-gamma (IFN-γ), Glyceraldehyde-3-phosphate dehydrogenase (GAPDH), Vascular Endothelial Growth Factor (VEGF), Fibronectin, Collagen type I (Col I), Matrix Metalloproteinase 8 (MMP8), and Matrix Metalloproteinase 1 (MMP1), were assessed following different treatments. RNA was extracted via the RNeasy Mini Kit (Qiagen, USA) based on the manufacturer's instructions. To synthesize cDNA from the purified RNA, the QuantiTect Reverse Transcription Kit (Qiagen, USA) was used. The primer sequences of genes are presented in Table 3. Real-time PCR was conducted by ABI Step One (Applied Biosystems, Sequence Detection Systems, Foster City, CA), and the Solis BioDyne kit was utilized to amplify cDNA fragments (5x hot firepole EvaGreen qPCR mix plus (ROX)). To normalize the expression levels of the genes, based on the comparative 2 $-\Delta\Delta Ct$ method, GAPDH was applied as the internal gene.

Statistical Analysis

The data were reported as the mean ± standard deviation (SD) value of three independent experiments. Data analysis was performed with one-way analysis of variance (ANOVA) and Tukey post hoc test via GraphPad Prism® version 5.01 software (GraphPad Software, USA). $P<0.05$ was considered statistically significant.

Results

Cell Viability Evaluation

Exposure of HGF cells to PBMT produced significant wavelength- and dose-dependent effects on viability. At 650 nm, irradiation with 4 J/cm² increased viability to ~130% of control, while 8 J/cm² further enhanced viability to ~160%. Both energy densities were statistically higher than the control ($P<0.01$ to $P<0.001$) (Figure 1A). At 810 nm, a graded response was observed; viability rose to ~120% at 4 J/cm², ~126% at 5.4 J/cm², ~138% at 8 J/cm², and ~140% at 8.1 J/cm² ($P<0.05$ to $P<0.001$) (Figure 1B). Combined irradiation at 650 and 810 nm demonstrated synergistic effects. Cells exposed to 8 J/cm² (both wavelengths simultaneously) achieved ~145% viability ($P<0.001$), while the 6.6 J/cm² group reached ~130% above the control ($P<0.001$) (Figure 1C). Taken together, PBMT promoted HGF viability in a wavelength- and dose-dependent manner, with the highest increases observed at 8 J/cm² in each group. These conditions, therefore, were selected for subsequent migration, cytokine, and gene expression experiments.

Cell Migration Evaluation

In line with viability outcomes, PBMT enhanced cell migration. Scratch assays revealed significantly accelerated wound closure in all groups at 24 and 48 hours compared to the control ($P<0.001$) (Figure 2). Although migration in the 810 nm group at 24 hours was comparable to the

Table 3. Primer sequences used for real-time PCR

Name	Forward Primer Sequence (5′→3′)	Reverse Primer Sequence (5′→3′)
INF-γ	GAGTGTGGAGACCATCAAGGAAG	TGCTTTGCGTTGGACATTCAAGTC
IL-6	AGACAGCCACTCACCTCTTCAG	TTCTGCCAGTGCCTCTTTGCTG
TNF-α	CTCTTCTGCCTGCTGCACTTTG	ATGGGCTACAGGCTTGTCACTC
MMP1	TCAGGGGAGATCATCGGGAC	GTTCATGAGCTGCAACACGATG
MMP8	ACCAACACCTCCGCAAATTACAAC	TCTTGGTCCAGTAGGTTGGATAG
Collagen I	ATGATGGGGAAGCTGGAAAAC	CAAACCACTGAAACCTCTGTGT
Fibronectin	ACTCTGTCAACGAAGGCTTGAAC	ACCACTTCCAAAGCCTAAGCAC
VEGF	TTGCCTTGCTGCTCTACCTCCA	GATGGCAGTAGCTGCGCTGATA
GAPDH	GTCTCCTCTGACTTCAACAGCG	ACCACCCTGTTGCTGTAGCCAA

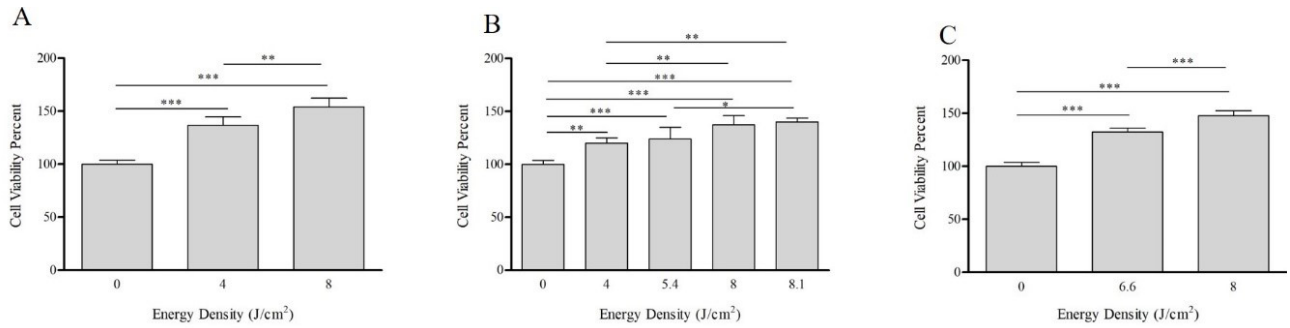

Figure 1. Analysis of HGF cell viability following exposure to different energy densities and 24-hour post-treatment culture. (A): Laser 650 nm (B): Laser 810 nm, and (C): Laser 650 + 810 nm. The results were reported as mean ± SD (n = 5) (**P < 0.01, ***P < 0.001)

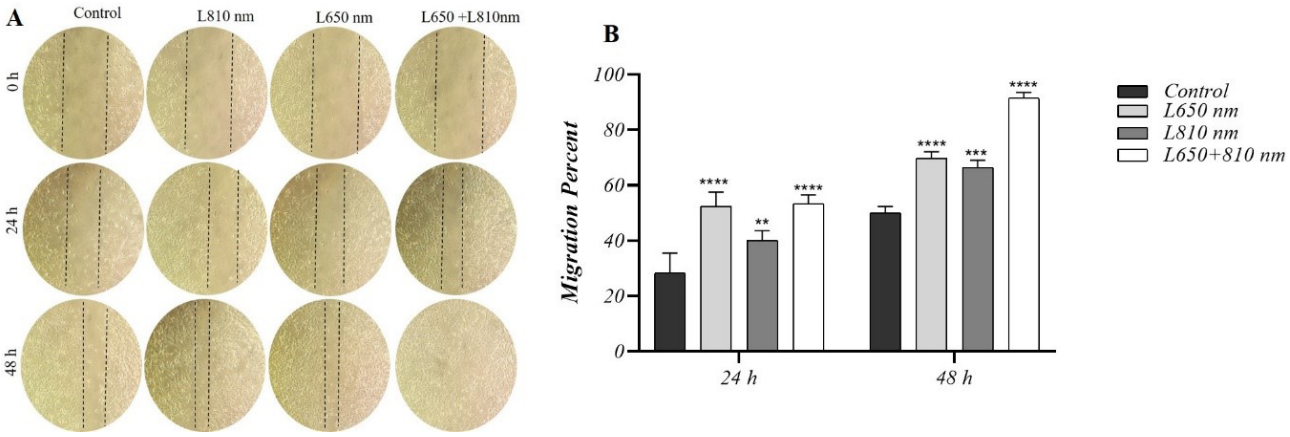

Figure 2. (A) Cell migration at 24 and 48 hours after scratching (B) Quantitative analysis of migration percentages in HGF cells following different laser exposure. The results were reported as mean ± SD (n = 3) (**P < 0.01, ***P < 0.001, ****P < 0.0001)

control, it still reached significance (P < 0.01). Importantly, the combined 650 + 810 nm groups demonstrated the most pronounced migration, suggesting an additive effect of dual-wavelength exposure. These findings support the link between increased viability and improved migratory capacity, both of which are key determinants of wound healing.

Cytokine Profiling Evaluation

Cytokine secretion was distinctly modulated by PBMT. At 810 nm, IFN-γ levels increased relative to the control (P < 0.05), while 650 nm treatment further elevated IFN-γ compared with both 810 nm (P < 0.01) and combined treatment groups (P < 0.05) (Figure 3A).

For IL-6 and TNF-α, irradiation at 810 nm increased concentrations compared with the control (P < 0.05). The 650 nm group exhibited even higher levels than the 810 nm group (P < 0.01), while combined treatment induced intermediate elevations (P < 0.05 vs control) (Figure 3B–C).

These results highlight wavelength-specific cytokine modulation, with 650 nm favoring greater inflammatory cytokine induction compared to 810 nm or dual treatment. This suggests that while both wavelengths activate immune mediators, their relative contributions differ.

Gene Expression Evaluation

Laser irradiation produced distinct and wavelength-specific changes in the expression of genes associated with immune regulation, extracellular matrix remodeling, and angiogenesis (Figure 4). Pro-inflammatory genes, including IFN-γ, IL-6, and TNF-α, were significantly upregulated across treatment groups, with the 650 nm group exhibiting the highest induction compared with the 810 nm ($P<0.0001$) group and the combined irradiation group ($P<0.001$). By contrast, MMP1 and MMP8, which mediate matrix degradation, were notably downregulated following 810 nm irradiation, suggesting reduced extracellular matrix breakdown; in the combined treatment group, expression levels of these genes increased relative to single-wavelength groups but remained lower than those in the control group. Genes linked to repair and angiogenesis, such as Collagen I, VEGF, and Fibronectin, were markedly upregulated following PBMT. Among these, the 810 nm group demonstrated the strongest increases relative to the control, while the 650 nm and combined groups also showed significant but comparatively lower expression. Notably, VEGF expression in the combined treatment group was significantly enhanced compared to the control ($P<0.0001$), highlighting a synergistic pro-angiogenic effect. Together, these findings reveal that PBMT exerts complementary and wavelength-dependent influences on gene regulation: 650 nm primarily drives inflammatory gene expression, 810 nm favors tissue stabilization and

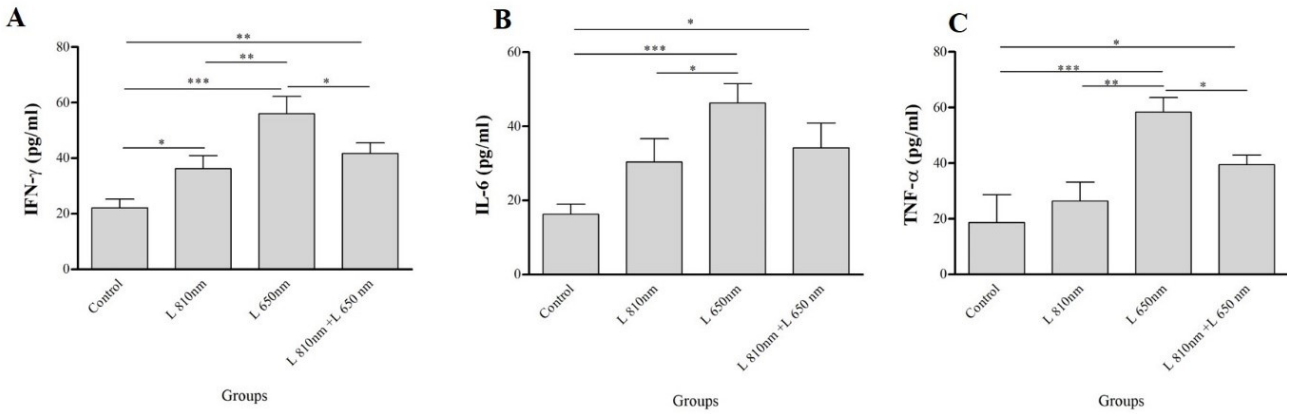

Figure 3. Statistical analysis of changes in inflammatory cytokine production (A: IFN-γ, B: IL-6, C: TNF-α) in human gingival fibroblasts using ELISA. The results were reported as mean ± SD (n = 3). (*$P<0.05$, **$P<0.01$, ***$P<0.001$)

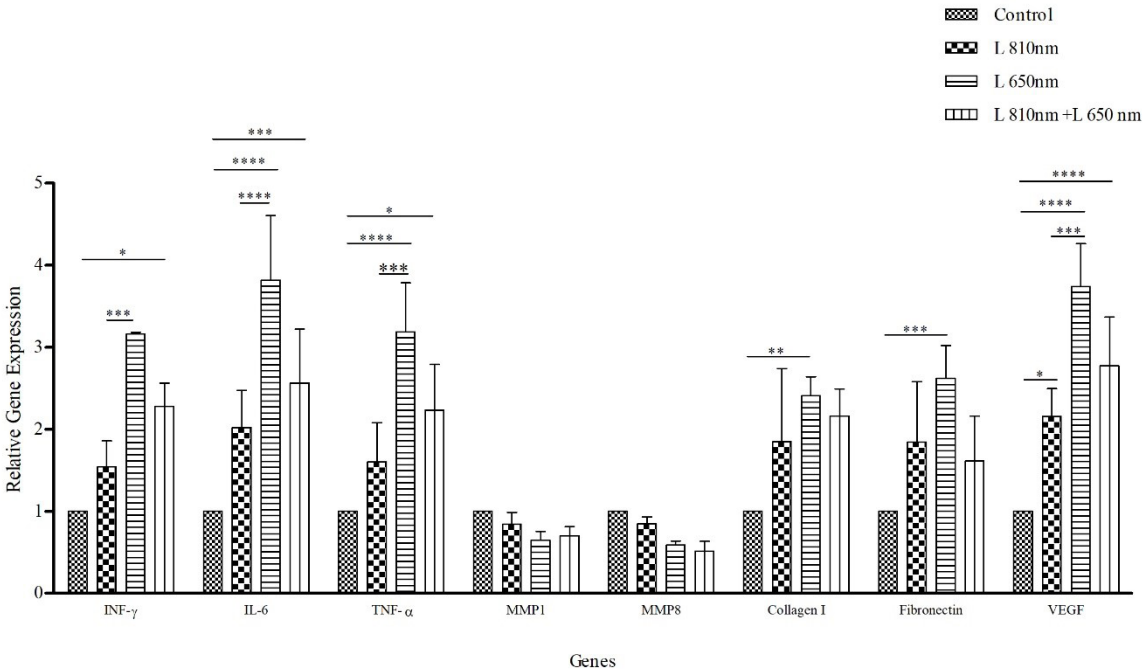

Figure 4. Relative mRNA expression levels of IFN-γ, IL-6, TNF-α, MMP1, MMP8, Collagen I, VEGF, and Fibronectin in human gingival fibroblasts following PBMT at 650 nm, 810 nm, or their combination, assessed by real-time PCR. Data are presented as mean ± SD (n = 3). Statistical significance compared with the control group: *$P<0.05$, **$P<0.01$, ***$P<0.001$, ****$P<0.0001$

angiogenic pathways, and combined irradiation integrates these responses to promote a balanced reparative profile.

Discussion

Epithelial and fibroblast cells are central to wound healing across tissues because of their ability to migrate into injured sites, proliferate, and release paracrine factors that stimulate underlying tissue layers. Our study demonstrated that PBMT at 650 and 810 nm enhanced viability, migration, cytokine secretion, and gene expression in HGFs, supporting its therapeutic role in wound repair. These results align with earlier research demonstrating that PBMT promotes proliferation and protein synthesis in HGFs, with a recent systematic review confirming significant increases in viability, migration, and growth factor release at red and near-infrared wavelengths.[15]

The biological effects observed in this study were distinctly wavelength-dependent. At 650 nm, PBMT strongly induced pro-inflammatory cytokines (IL-6, TNF-α, IFN-γ), which may represent an early immune activation phase. This priming effect is important for initiating the wound-healing cascade, as transient inflammation facilitates subsequent tissue repair. Conversely, 810 nm irradiation reduced MMP1 and MMP8 expression, while enhancing VEGF, Fibronectin, and Collagen I. This pattern suggests that NIR wavelengths preferentially promote extracellular matrix stabilization and angiogenesis. The combined 650 + 810 nm irradiation produced the most robust improvements in viability and migration, suggesting a complementary mechanism: Red light initiates inflammatory and proliferative cues, while NIR supports matrix remodeling and angiogenesis.[16,17]

Our findings align with and extend prior work. As an example, Karoussis et al found that 810 nm irradiation at 12 J/cm² maximized HGF proliferation and upregulated Collagen I, VEGF, and EGF expression.[18] Similarly, Cardoso et al showed that PBMT could counteract the cytokine-induced suppression of proliferation and migration in HGFs, while increasing VEGF and EGF.[19] These data support our observation that PBMT restores fibroblast function even under inflammatory stress. Furthermore, Pansani et al demonstrated that PBMT reduced IL-6 and IL-8 secretion while increasing VEGF in fibroblasts cultured on titanium and zirconia,[20] reinforcing the modulatory capacity of PBMT on cytokine balance. In line with our MMP findings, PBMT has also been shown to suppress MMP-2 and MMP-9 activity in TNF-α–stimulated fibroblasts,[19] confirming its matrix-protective effects.

Angiogenic signaling appears particularly responsive to NIR irradiation. Both 660 nm and 808 nm irradiation significantly increased VEGF expression in HGFs, with stronger effects at 808 nm,[21] which is consistent with our results showing VEGF upregulation after 810 nm PBMT. Other studies also confirm that lower red and blue ranges (635 nm and 405 nm) can increase fibroblast proliferation, [22] while Nd:YAG (neodymium-doped yttrium aluminum garnet; Nd:$Y_3Al_5O_{12}$) PBMT at 1064 nm can stimulate proliferation and EGF secretion.[23] Together, these results highlight the broad potential of PBMT across multiple spectral bands, though the precise biological responses depend on wavelength, dose, and cellular context.

Mechanistically, PBMT is thought to act primarily via cytochrome c oxidase (CCO) in the mitochondrial respiratory chain, resulting in enhanced ATP synthesis, the regulation of reactive oxygen species (ROS), and the activation of transcription factors responsible for controlling cytokines and growth factors. These molecular events explain the observed increases in VEGF, collagen synthesis, and inflammatory mediators, and may underlie the distinct gene signatures we identified for 650 nm versus 810 nm irradiation. For example, ROS at lower levels function as secondary messengers promoting proliferation and angiogenesis, while excessive ROS could trigger apoptosis. Thus, the balance achieved by appropriate PBMT dosing appears critical for optimizing therapeutic outcomes. The novelty of our study lies in its direct head-to-head comparison of 650 nm, 810 nm, and combined PBMT, while simultaneously evaluating multiple outcomes, cell viability, migration, cytokine secretion, and gene expression. This integrated approach allows us to identify distinct wavelength-specific gene signatures and demonstrate that dual-wavelength PBMT produces complementary, potentially synergistic benefits. Unlike most prior studies, which tested single wavelengths or limited biological endpoints, our work provides a more comprehensive profile of PBMT effects in HGFs. From a translational perspective, these findings have relevance for periodontal regeneration, wound closure after oral surgery, and peri-implant healing. Optimizing PBMT protocols could accelerate gingival repair, enhance angiogenesis, and improve integration of biomaterials. Moreover, tailoring PBMT by wavelength and dose could allow clinicians to direct biological responses toward inflammation control, matrix remodeling, or angiogenesis, depending on the clinical need. Nevertheless, this study has certain limitations. The experiments were performed in vitro with a single cell type and limited time points. Fibroblasts interact dynamically with keratinocytes, endothelial cells, and immune cells during wound healing, and these interactions cannot be fully captured in monoculture. In addition, long-term effects and repeated dosing regimens were not addressed. Future research should expand to co-culture and 3D models, test PBMT in animal wound-healing models, and evaluate outcomes in controlled clinical trials to establish standardized treatment protocols.[24,25]

Conclusion

In conclusion, PBMT showed wavelength-dependent effects on human gingival fibroblasts. Irradiation at 650

nm primarily activated pro-inflammatory mediators, while 810 nm promoted extracellular matrix remodeling and angiogenesis through VEGF, Fibronectin, and Collagen I upregulation with MMP downregulation. Dual-wavelength treatment produced synergistic improvements in cell viability and migration, highlighting complementary roles of red and NIR light. These findings emphasize PBMT's potential as a tunable therapy for periodontal regeneration, oral wound healing, and implant integration, warranting further validation in advanced models and clinical trials.

Acknowledgments
The authors thank Zist Pajooh Afra Company for their help and support during this research.

Authors' Contribution
Conceptualization: Jaber Zafari.
Data curation: Danial Khayatan.
Formal analysis: Jaber Zafari.
Investigation: Fatemeh Javani Jouni.
Methodology: Jaber Zafari.
Project administration: Fatemeh Javani Jouni.
Resources: Leila Mohaghegh Shalmani.
Software: Leila Mohaghegh Shalmani.
Supervision: Fatemeh Javani Jouni.
Validation: Hossein Vazin.
Visualization: Hossein Vazin.
Writing–original draft: Danial Khayatan.
Writing–review & editing: Fatemeh Javani Jouni.

Competing Interests
There is no conflict of interest.

Ethical Approval
This research was approved by the ethics committee of Shahid Beheshti University of Medical Sciences (reference number: IR.SBMU.RETECH.REC.1401.155).

Funding
This work was supported by the Laser Application in Medical Sciences Research Center, Shahid Beheshti University of Medical Sciences.

References
1. Wilkinson HN, Hardman MJ. Wound healing: cellular mechanisms and pathological outcomes. Open Biol. 2020;10(9):200223. doi: 10.1098/rsob.200223.
2. Frykberg RG, Banks J. Challenges in the treatment of chronic wounds. Adv Wound Care (New Rochelle). 2015;4(9):560-82. doi: 10.1089/wound.2015.0635.
3. Cotler HB, Chow RT, Hamblin MR, Carroll J. The use of low-level laser therapy (LLLT) For Musculoskeletal Pain. MOJ Orthop Rheumatol. 2015;2(5):00068. doi: 10.15406/mojor.2015.02.00068.
4. de Oliveira MF, Johnson DS, Demchak T, Tomazoni SS, Leal-Junior EC. Low-intensity LASER and LED (photobiomodulation therapy) for pain control of the most common musculoskeletal conditions. Eur J Phys Rehabil Med. 2022;58(2):282-9. doi: 10.23736/s1973-9087.21.07236-1.
5. Kobayashi H, Choyke PL. Near-infrared photoimmunotherapy of cancer. Acc Chem Res. 2019;52(8):2332-9. doi: 10.1021/acs.accounts.9b00273.
6. Desmet KD, Paz DA, Corry JJ, Eells JT, Wong-Riley MT, Henry MM, et al. Clinical and experimental applications of NIR-LED photobiomodulation. Photomed Laser Surg. 2006;24(2):121-8. doi: 10.1089/pho.2006.24.121.
7. Wu S, Liang H, Li Y, Zou W, Liao Z, Wang W, et al. Novel broadband NIR phosphors Y(2)Mg(2)Ga(2)Si(2)O(12):xCr(3+) for NIR LED applications. Dalton Trans. 2023;52(19):6569-77. doi: 10.1039/d3dt00469d.
8. Mignon C, Uzunbajakava NE, Castellano-Pellicena I, Botchkareva NV, Tobin DJ. Differential response of human dermal fibroblast subpopulations to visible and near-infrared light: Potential of photobiomodulation for addressing cutaneous conditions. Lasers Surg Med. 2018;50(8):859-82. doi: 10.1002/lsm.22823.
9. Rybak D, Rinoldi C, Nakielski P, Du J, Haghighat Bayan MA, Zargarian SS, et al. Injectable and self-healable nano-architectured hydrogel for NIR-light responsive chemo- and photothermal bacterial eradication. J Mater Chem B. 2024;12(7):1905-25. doi: 10.1039/d3tb02693k.
10. Zi X, Zhang G, Qiu S. Up-regulation of LINC00619 promotes apoptosis and inhibits proliferation, migration and invasion while promoting apoptosis of osteosarcoma cells through inactivation of the HGF-mediated PI3K-Akt signalling pathway. Epigenetics. 2022;17(2):147-60. doi: 10.1080/15592294.2021.1890873.
11. Arini AP, Namangkalakul W, Limraksasin P, Osathanon T. Effects of lactalbumin enzymatic hydrolysate on human squamous cell carcinoma cells-an in vitro study. J Oral Biol Craniofac Res. 2024;14(2):222-9. doi: 10.1016/j.jobcr.2024.02.011.
12. Peng X, Liu Y, Zhu S, Peng X, Li H, Jiao W, et al. Co-targeting PI3K/Akt and MAPK/ERK pathways leads to an enhanced antitumor effect on human hypopharyngeal squamous cell carcinoma. J Cancer Res Clin Oncol. 2019;145(12):2921-36. doi: 10.1007/s00432-019-03047-2.
13. Nguyen PA, Pham TAV. Effects of platelet-rich plasma on human gingival fibroblast proliferation and migration in vitro. J Appl Oral Sci. 2018;26:e20180077. doi: 10.1590/1678-7757-2018-0077.
14. Everts PA, Lana JF, Onishi K, Buford D, Peng J, Mahmood A, et al. Angiogenesis and tissue repair depend on platelet dosing and bioformulation strategies following orthobiological platelet-rich plasma procedures: a narrative review. Biomedicines. 2023;11(7):1922. doi: 10.3390/biomedicines11071922.
15. Giannini R, Vassalli M, Chellini F, Polidori L, Dei R, Giannelli M. Neodymium:yttrium aluminum garnet laser irradiation with low pulse energy: a potential tool for the treatment of peri-implant disease. Clin Oral Implants Res. 2006;17(6):638-43. doi: 10.1111/j.1600-0501.2006.01278.x.
16. Marashian SM, Hashemian M, Pourabdollah M, Nasseri M, Mahmoudian S, Reinhart F, et al. Photobiomodulation improves serum cytokine response in mild to moderate COVID-19: the first randomized, double-blind, placebo controlled, pilot study. Front Immunol. 2022;13:929837. doi: 10.3389/fimmu.2022.929837.
17. Pasternak-Mnich K, Kujawa J, Agier J, Kozłowska E. Impact of photobiomodulation therapy on pro-inflammation functionality of human peripheral blood mononuclear cells - a preliminary study. Sci Rep. 2024;14(1):23111. doi: 10.1038/s41598-024-74533-y.
18. Karoussis IK, Kyriakidou K, Psarros C, Afouxenides P, Vrotsos IA. Dosage effects of an 810 nm diode laser on the proliferation and growth factor expression of human gingival fibroblasts. J Lasers Med Sci. 2021;12:e25. doi: 10.34172/jlms.2021.25.
19. Cardoso LM, Pansani TN, Hebling J, de Souza Costa CA, Basso FG. Photobiomodulation of inflammatory-cytokine-related effects in a 3-D culture model with gingival fibroblasts.

Lasers Med Sci. 2020;35(5):1205-12. doi: 10.1007/s10103-020-02974-8.
20. Pansani TN, Basso FG, Turirioni AP, Kurachi C, Hebling J, de Souza Costa CA. Effects of low-level laser therapy on the proliferation and apoptosis of gingival fibroblasts treated with zoledronic acid. Int J Oral Maxillofac Surg. 2014;43(8):1030-4. doi: 10.1016/j.ijom.2014.02.011.
21. Kocherova I, Bryja A, Błochowiak K, Kaczmarek M, Stefańska K, Matys J, et al. Photobiomodulation with red and near-infrared light improves viability and modulates expression of mesenchymal and apoptotic-related markers in human gingival fibroblasts. Materials (Basel). 2021;14(12):3427. doi: 10.3390/ma14123427.
22. Sterczała B, Grzech-Leśniak K, Michel O, Trzeciakowski W, Dominiak M, Jurczyszyn K. Assessment of human gingival fibroblast proliferation after laser stimulation in vitro using different laser types and wavelengths (1064, 980, 635, 450, and 405 nm)-preliminary report. J Pers Med. 2021;11(2):98. doi: 10.3390/jpm11020098.
23. Gkogkos AS, Karoussis IK, Prevezanos ID, Marcopoulou KE, Kyriakidou K, Vrotsos IA. Effect of Nd:YAG low level laser therapy on human gingival fibroblasts. Int J Dent. 2015;2015:258941. doi: 10.1155/2015/258941.
24. Ohsugi Y, Niimi H, Shimohira T, Hatasa M, Katagiri S, Aoki A, et al. In vitro cytological responses against laser photobiomodulation for periodontal regeneration. Int J Mol Sci. 2020;21(23):9002. doi: 10.3390/ijms21239002.
25. Lee KD, Chiang MH, Chen PH, Ho ML, Lee HZ, Lee HE, et al. The effect of low-level laser irradiation on hyperglycemia-induced inflammation in human gingival fibroblasts. Lasers Med Sci. 2019;34(5):913-20. doi: 10.1007/s10103-018-2675-6.